REPORT DOCUMENTATION PAGE

Form Approved
OMB No. 0704-0188

(2)

...tion is estimated to average 1 hour per response, including the time for reviewing instructions, searching existing data sources, ...pleting and reviewing the collection of information. Send comments regarding this burden estimate or any other aspect of this ... for reducing this burden to Washington Headquarters Services, Directorate for Information Operations and Reports, 1215 Jefferson ...ington, VA 22202-4302, and to the Office of Management and Budget, Paperwork Reduction Project (0704-0188), Washington, DC 20503.

1. AGENCY USE ONLY (Leave blank)	2. REPORT DATE 27 Jan 93	3. REPORT TYPE AND DATES COVERED Final Report 15 May 89 - 29 Mar 92

4. TITLE AND SUBTITLE

Experimetal and theoretical studies of proximity effect and coulbmb blockade phenomena in Josephson junctions

5. FUNDING NUMBERS

2305/C3

6. AUTHOR(S)

Profess El. L. Wolf

7. PERFORMING ORGANIZATION NAME(S) AND ADDRESS(ES)

Polytechnic University
333 Jay Street
Brooklyn, NY 11201

8. PERFORMING ORGANIZATION REPORT NUMBER

AFOSR-TR- 93 0105

9. SPONSORING/MONITORING AGENCY NAME(S) AND ADDRESS(ES)

AFOSR/NE
110 Duncan Avenue, Suite B115
Bolling AFB, DC 20332-0001

10. SPONSORING/MONITORING AGENCY REPORT NUMBER

AFOSR-89-0338

11. SUPPLEMENTARY NOTES

12a. DISTRIBUTION/AVAILABILITY STATEMENT

APPROVED FOR PUBLIC RELEASE; DISTRIBUTION IS UNLIMITED.

12b. DISTRIBUTION CODE

13. ABSTRACT (Maximum 200 words)

The topics of theoretical and experimental interest in this research have been: Behavior of ultrasmall low capacitance (Coulbomb-blockaded) Josephson and normal metal tunnel junction microstructures. Experimentally the microstructures (STM). A particular interest is in the fundamentally new mechanisms of interaction with radiation believed to operate in these systems. The Proximity Induced Josephson Effect (PIJE), an effect occurring at a Normal Metal/Superconductor (N/S) interface which displays many of the features of the Josephson effect, and whose device potential has not been at all explored. Related topics in our research in this project have been methods to form Josephson junctions using cuprate superconductors, and methods to prepare and modify the surface of cuprate superconductors to make Josephson junctions and other electronic devices.

14. SUBJECT TERMS	15. NUMBER OF PAGES
	16. PRICE CODE

17. SECURITY CLASSIFICATION OF REPORT	18. SECURITY CLASSIFICATION OF THIS PAGE	19. SECURITY CLASSIFICATION OF ABSTRACT	20. LIMITATION OF ABSTRACT
UNCLASSIFIED	UNCLASSIFIED	UNCLASSIFIED	UL (UNLIMITED)

NSN 7540-01-280-5500
Standard Form 298 (Rev 2-89)
Prescribed by ANSI Std 239-18
298-102

POLYTECHNIC UNIVERSITY

DEPARTMENT OF PHYSICS

Final Technical Report, AFOSR Grant 89-0338

Title: "Experimental and Theoretical Studies of Proximity Effect and Coulomb Blockade Phenomena in Josephson Junctions", E. L. Wolf and B. Laikhtman, PI's, Department of Physics, Polytechnic University, Six Metrotech Center, Brooklyn, NY 11201

Prepared January 27, 1993 by E. L. Wolf ELWolf

I. Introduction

The topics of theoretical and experimental interest in this research have been:

Behaviour of ultrasmall low capacitance (Coulomb-blockaded) Josephson and normal metal tunnel junction microstructures. Experimentally the microstructures are formed/studied us cryogenic Scanning Tunneling Microscopes (STM). A particular interest is in the fundamentally new mechanisms of interaction with radiation believed to operate in these systems.

The Proximity Induced Josephson Effect (PIJE), an effect occurring at a Normal Metal/Superconductor (N/S) interface which displays many of the features of the Josephson effect, and whose device potential has not been at all explored.

Related topics in our research in this project have been methods to form Josephson junctions using cuprate superconductors, questions of magnetic field and vortex interactions and losses in the surface of cuprate superconductors, and methods to prepare and modify the surface of cuprate superconductors to make Josephson junctions and other electronic devices.

II. Results

In the STM based study of Coulomb blockaded Josephson junctions, our work [1,2] was based on the concept of the double tunneling capacitor, formed using the STM. A small particle present on a (partially oxidized) metallic substrate can exhibit small capacitances and small electron tunneling rates to both the STM tip and the underlying substrate. In these structures the interelectrode capacitances can be on the order of 10^{-17} F, corresponding to a single electron charging energy of $e/C = 16$ meV, a significant energy at e.g. 4.2 K where kT is 0.36 meV. For a single tunneling capacitor with current feed and voltages and kT/e much less than e/C a regime of sequential temporally correlated electron hopping was predicted [3], with the characteristic frequency I/e, I the tunnel current. The possibility of interaction of the correlated tunneling events in this regime with microwave radiation of the matching frequency is of interest. With K-band microwaves at 25GHz, the level of I is 4 nA, a typical STM current level. Microwave correlation experiments in the double junction case are also of interest. As an approach to this problem we built and tested a unique microwave cryogenic STM.[4,5], illustrated in Fig. 1.

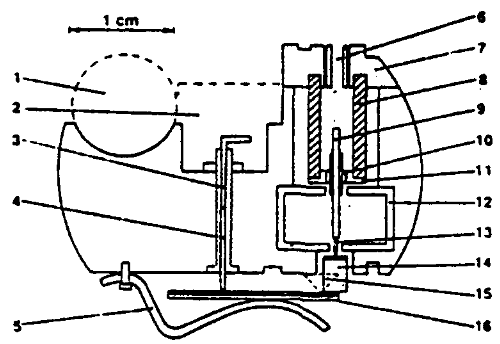

FIG 1

Fig. 1. Low temperature STM cross section: (1) worm, (2) wheel, (3) 0000-160 threaded rod, (4) stainless steel foot-pusher, (5) Be-Cu spring, (6) 0-80 coarse-adjustment screw, (7) removable top piece, (8) piezoelectric tube scanner, (9) concentric stainless steel tube, (10) 4-40 stainless steel screw, (11) Macor ring, (12) waveguide, (13) tip, (14) copper sample mounting block with sample, (15) pivot feet, (16) semicircular bimorph disc.

The basic feature of this is that the STM tip traverses the narrow face of a K-band waveguide, and is thus parallel with the microwave E-field. In this way a microwave voltage appears between tip and sample as desired to stabilize the correlated electron tunneling events. In this design great rigidity is achieved by mounting tip and sample on a heavy metal base which encloses the stainless steel waveguide. The tip is mounted on the end of a piezotube mounted above the broad face of the guide. The piezo tube mount allows rough positioning of the tip across the guide, and in operation provides the transverse x,y motion of the tip in STM scanning. The fine z-spacing is accomplished on the opposite side of the guide by mounting the sample on a half circular piezo disk which flexes into a drumhead mode when the electrodes are biased. Convenient sample mounting is accomplished simply by removing the piezo half circular disk from its spring mounting.

An external adjustment of the z-spacing is accomplished by a worm driving a 20 tooth gear, advancing a 1/160 thread, which in turn pivots the piezo half disk on pivot feet of adjustable positions, providing 1/10th, 1/5th or 1/2 reduction of the motion. To reach tunneling distance, about 10 Angstroms, a stepping motor advances the worm gear via the drive rod from the outside, until stopped by the computer control system's detection of tunneling current. The resonant frequency of the cavity can also be adjusted from outside the dewar, by means of adjusting the endwall position. Figure 1 shows the design features of the microwave STM and is part of the paper [5] published in J. Physics E.

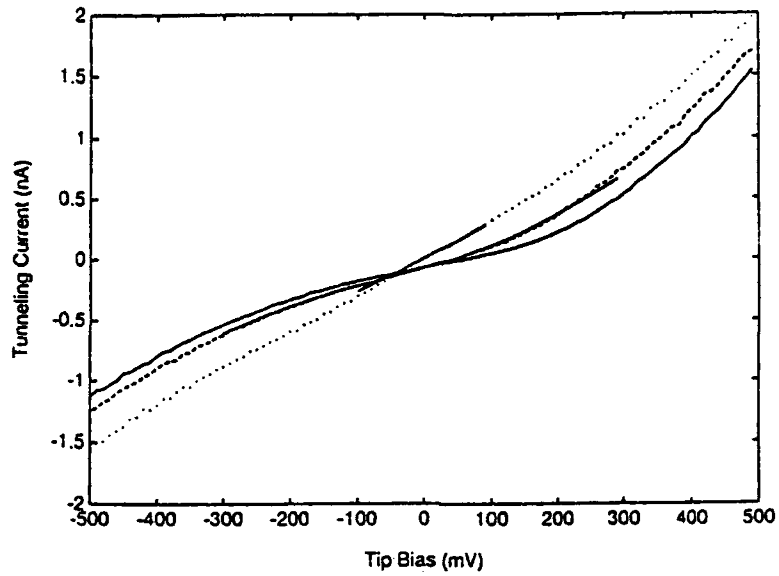

FIG 2

Fig 2. Microwave coupling to initially non-linear IV curve (full solid curve, -20dB) obtained at room temperature in microwave STM. Dashed curve (-16dB) shows partially linearized result, followed by dotted curve -6dB. The solid line segments are obtained numerically by averaging the initial curve over microwave sinusoidal voltages of 200 and 400 mV amplitudes, respectively. This demonstrates that the available microwave voltage between tip and sample can be as large as 400 mV.

Fig. 2 demonstrates that the microwave STM we have built provides a significant microwave voltage across tip and sample. An initially nonlinear I(V) is shown in the solid curve; increasing microwave power is seen to linearize the curves (-16 dB, dashed, with solid modeling section b; -6dB dotted with modeling section a). It appears that the microwave voltage available is in the range of several hundred millivolts at 25 GHz using this unique apparatus. A superinsulated helium cryostat has been set up for use with this microwave cryogenic STM.

The basic manifestation of the Proximity Induced Josephson Effect (PIJE) is a sharp non-linearity in the I-V curve of an N-I-S tunnel contact, which looks like a Josephson junction with a small series resistance. Other Josephson like aspects of the behaviour are the Fraunhofer-like $I_c(B)$, and Shapiro steps of voltage spacing hf/2e. We have published theoretical work relating experimental results [6,7] to the theory of Geshkenbein and Sokol [8]; a paper [9] has been published summarizing our findings. The conclusion drawn is that the PIJE effect indeed arises by the formation of a proximity induced superconducting layer in the N material, as supposed earlier. However, it appears that an AC current obeying the condition 2eV=hf is not to be expected, that the RF steps arise in a different manner, and that the qualitative aspect of the I(V) changes smoothly from a sharp nonlinearity closely resembling an RSJ model Josephson junction to a weak and broad excess current much as observed in the Pair Field Susceptibility work of Goldman and collaborators [10, 11, 12]. The suggestion that these disparate effects arise in the same way is we believe important and deserves extensive new experiments. Recent results by Agrit, Rodrigo and Viera [] have claimed to verify the effect and also an interpretation along the lines we proposed, specifically not to include a phase slip center.

Under the present grant we have designed and built a point contact tunneling apparatus with microwave coupling. This work was interrupted due to the loss of the researcher; and was carried on again in the fall of 1992. The first experiments performed with this new apparatus are shown in Fig. 3 and Fig. 4.

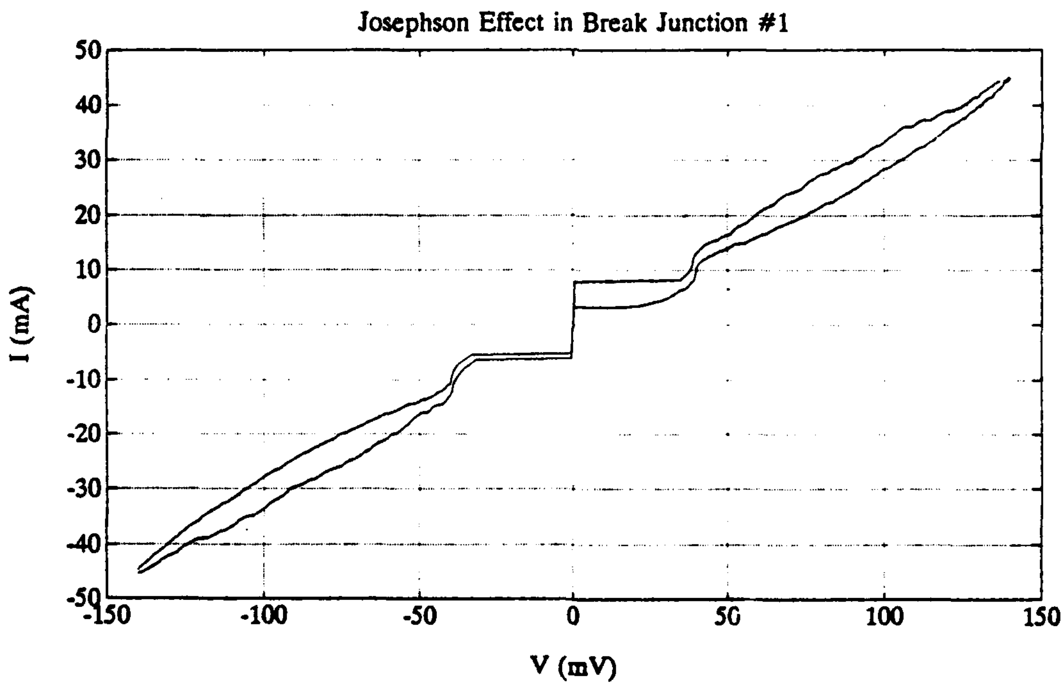

Fig. 3. Current voltage curve obtained at 4.2K with BSCCO SIS Josephson junction created by fracture of a single crystal in situ. The features of interest are a strong Josephson supercurrent, appreciable hysteresis, and a sharp quasiparticle current rise locating the sum gap.

These results were obtained using the new apparatus in a break junction mode, in which the point contact tip advance mechanism was used alternatively to bend a ceramic bar substrate on which a thin cuprate superconductor single crystal of $Bi_2Sr_2CaCu_2O_8$ (BSCCO) was cemented. Flexing of the ceramic substrate causes the cuprate to break under tensile stress, creating a cuprate\liquid helium\cuprate SIS Josephson junction. The coupling strength of the junction can be adjusted with the tip advance screw making use of the elasticity of the substrate which remains unbroken. The apparatus will allow microwave irradiation of such a junction, but that has not been done as yet.

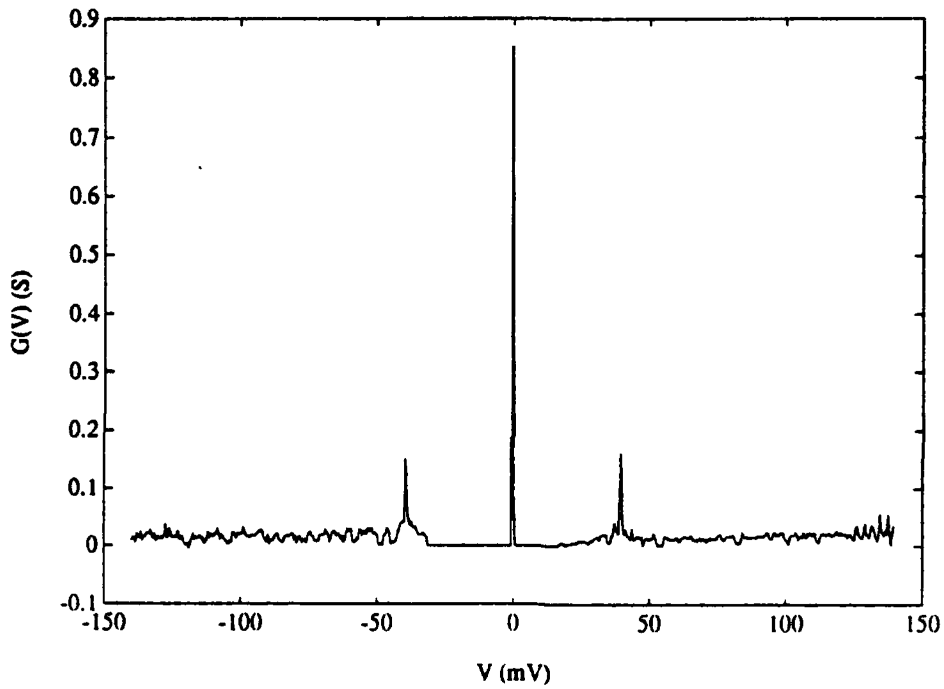

Fig. 4. Derivative of the I(V) curve shown in Fig. 3, revealing sharpness of the quasiparticle sum gap edge in this cuprate SIS break junction.

The data of Fig. 3 and Fig. 4, as yet unpublished, show for the first time a robust Josephson current, a very sharp sum gap response and an appreciable hysteresis. The earlier work [14,15] on BSCCO break junctions has not shown a Josephson current, and the quasiparticle peaks in G(V) are very broad rather than being sharp as in Fig 4.

Scanning Tunneling Microscope (STM) and UHV surface analysis work has been initiated with the goals of finding methods to pattern the BSCCO superconductor on a 100Å scale, and also to find methods of doping the material to change its hole concentration and superconducting properties. This work is stimulated by our recent demonstration [16] that the cryogenic Scanning Tunneling Microscope (CSTM) is capable of mapping the energy gap of a cuprate superconductor on a scale of 5Å. These observations [16] make clear that under attainable conditions superconductivity can exist in the first atomic layers of the specimen, which is very encouraging for the prospect of making superconducting devices.

We have grown single crystals of the cuprate $Bi_2Sr_2CaCu_2O_8$ (Bi2212) routinely, and have made extensive STM measurements at room temperature and at 4.2K on ab plane cleavage faces of this material, where a and b unit cell dimensions are 5.4Å. In this layerlike material, the basic unit is 15.4Å thick along the c-direction, a sandwich of the form BiO-SrO-CuO_2-Ca-CuO_2-SrO-BiO, two of which stack to make up the 30.8AÅ unit cell. We think of this as a .. = N-I-S-I-N = N-I-S-I-N = .. junction superlattice structure along the c-direction with period 15.4Å, where = represents a relatively high tunnel barrier across the van der Waals bond, I represents the internal barrier comprised by the SrO plane, S represents the double plane CuO_2 structure and N represents the BiO layer exposed by cleavage when the = barrier (weak bond) ruptures. In in-situ vacuum cleaved samples we can see the Bi atoms with nearest neighbor spacing 3.8Å.

In samples that are air-cleaved and quickly immersed in liquid He with our CSTM we have been able to make a mapping of the energy gap on the ab plane of the material. The energy gap as measured along a 500Å line is shown in Fig.5 [16] which demonstrates the 5Å resolution of our LDOS measurements.

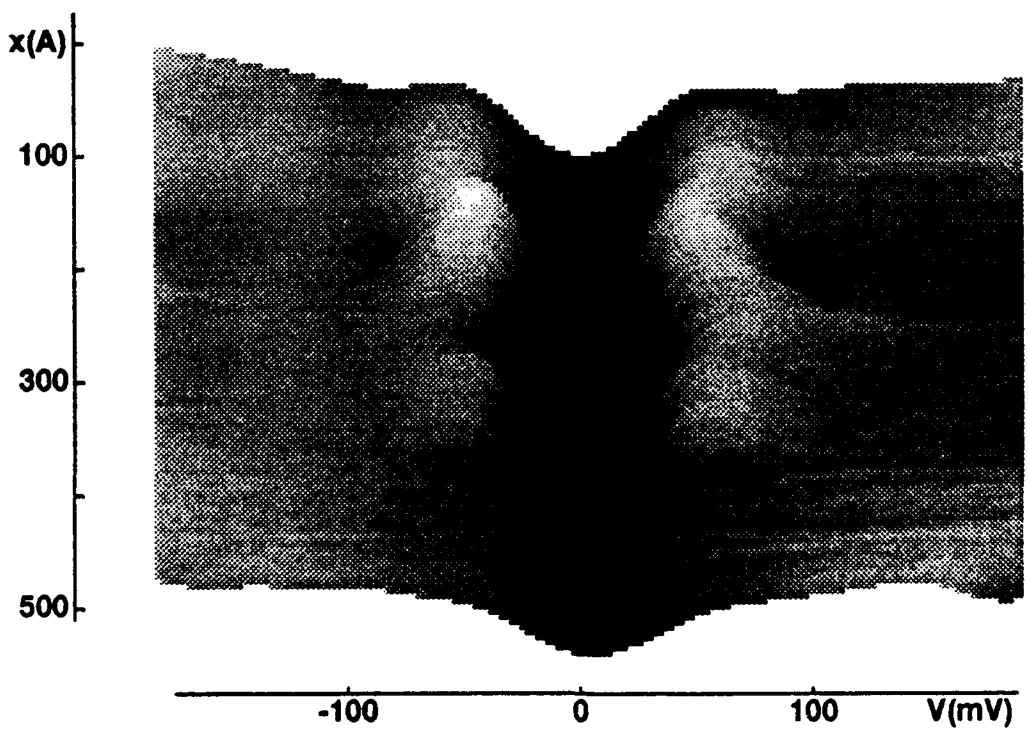

FIG. 5

GRAY SCALE DI/DV

We have found that the STM can be used as a patterning tool on the ab plane of the cuprate superconductor. Successive layers of the material can be removed by rastering the tip under bias conditions not far different from those normally used in scanning to provide topography.

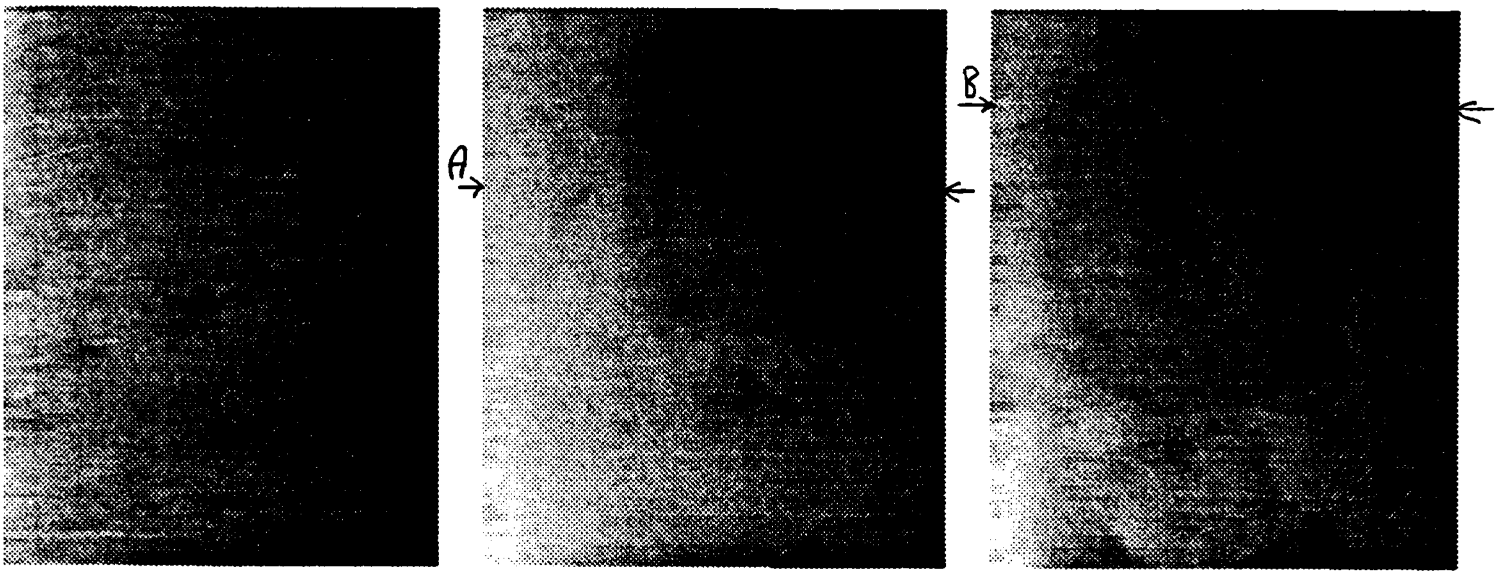

FIG. 6A **B** **C**

In Fig. 6 ABC are a sequence of topographs made at room temperature in our small air-helium STM. A square region 1000x1000 $(\text{Å})^2$is being successively raster scanned, with 500 pA current and 0.5 Volt bias. As this process proceeds, a square hole (B) is seen to appear in the scanned region, with some double removal in (C). This is an STM etching process, the mechanism of which is not yet known, but may be related simply to local heating related to the current density, $500\ 10^{-12}\text{A}/(5\ 10^{-8}\text{cm})^2=2\ 10^5\ \text{A/cm}^2$, taking the effective dimension of the current "beam" as 5Å.

Line scans across images (B) and (C) shown in Fig. 7 AB indicate the sharp-edged "wells" that have been etched have depths close to one full c-lattice constant, 30.8Å, as one might expect. We also have some evidence of etching to half this distance. There is also evidence for a second step of the etching process, which would produce a well 61.6Å deep. This provides a method for etching patterns into the 2212 surface, and we see no reason why a circular trench cannot be etched, isolating a 100-1000Å diameter "pillar" or "quantum dot" of 2212.

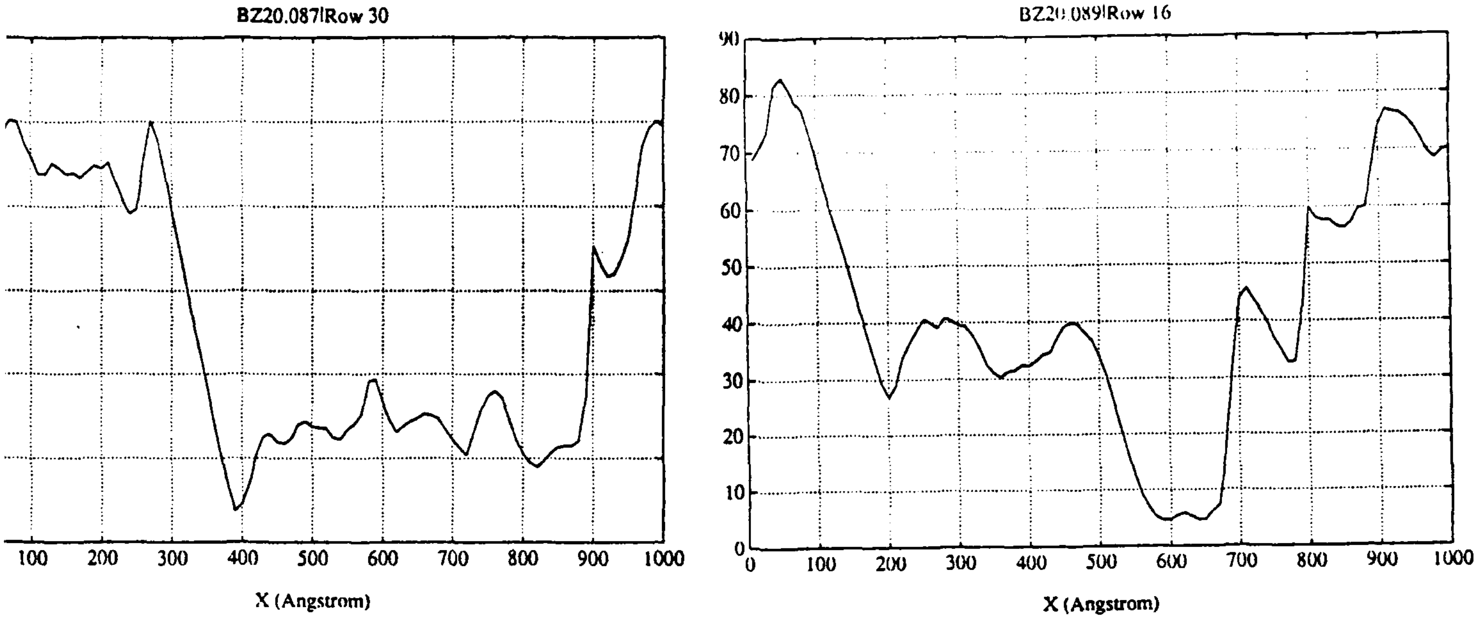

FIG. 7A **B**

Theoretical work has also been carried out under the present grant on electron-device-related aspects of layered superconductors such as BSCCO. These calculations are related to the response of the superconductor to electromagnetic fields, specifically the microwave absorption [17]. An aspect of real superconductors which is of concern and interest in computer applications is flux trapping. In state of the art conceptions of superconducting logic devices, the RFSQ logic proposed by Likharev and Semonov [18], stray magnetic field from even single trapped flux quanta will be problematic. A second calculation performed under the present support [19] considers the thermal formation of vortex loops in layered superconductors such as BSSCO. It is predicted that flux loops may appear thermally near T_c, which is consistent with several recent papers [20,21] relating to thermal generation of flux lines in similar circumstances. In the present paper [19], which has been submitted to Phys. Rev. Lett., a suggestion is made that such magnetic vortices, if frozen in or quenched by a rapid sample cooling, may lead to local variations in the superconducting energy gap as we have observed and shown in Fig. 5 [16]. These two papers [17,19], at present submitted but not published, are attached to the present report as Appendix A and Appendix B, respectively.

References and Publications (P)

1. (P) B. Laikhtman and E. L. Wolf, "Tunneling Time and Effective Capacitance for Single Electron Tunneling", Physics Lett. A 139, 257 (1989)

2. Z. Y. Rong, L. F. Cohen, and E. L. Wolf, "Scanning Tunneling Microscope Observations of the Coulomb Blockade", Phys. Lett. A146, 281 (1990).

3. K. K. Likharev, "Correlated Discrete Transfer of Single Electrons in Ultrasmall Tunnel Junctions", IBM J. Res. Devel. 32 144 (1988).

4. (P) L. F. Cohen and E. L. Wolf, "Low Temperature Microwave Scanning Tunneling Microscope", Bull. Am. Phys. Soc. 35, 802 (1990).

5. (P) L. F. Cohen and E. L. Wolf, "Microwave Coupled Cryogenic STM", Meas. Sci. Technol 2 83 (1991).

6. S. Han, K. W. Ng, E. L. Wolf, H. F. Braun, L. Tanner, Z. Fisk,J. L. Smith, and M. R. Beasley, Phys. Rev. B32 7467 (1985).

7. E. L. Wolf, S. Han, Z. G. Khim, K. W. Ng, A. J. Millis, J. L. Smith, Z. Fisk, J. Appl. Phys. 61, 3899 (1987).

8. V. B. Geshkenbein and A. V. Sokol, Sov. Phys. JETP 67,362 (1988).

9. S. Han, L. F. Cohen and E. L. Wolf, "Apparent Critical Currents and RF Steps in a Second Order Proximity Induced Josephson Effect", Phys. Rev. B. 42 8682 (1990).

10. J. T. Anderson and A. M. Goldman, Phys. Rev. Lett. 25, 743 (1970).

11. A. M. Kadin and A. M. Goldman, Phys. Rev. B25 6701 (1982).

12. A. M. Kadin, Phys. Rev. B41, 4072 (1990).

13. N. Agrait, J. G. Rodrigo, and S. Vieira, "Transition from the tunneling regime to point contact and proximity-induced Josephson effect in lead-normal-metal nanojunctions", Phys. Rev. B 46 5814, (1992).

14. D. Mandrus, L. Forro, D. Koller and L. Mihaly, Nature 351 460 (1991).

15. T. Becherer, J. Kowalewski, M. Schmitt, M. Huth, W. Assmus, and H. Adrian, "Break Junction Tunneling on $Bi_2Sr_2CaCu_2O_8$-Single Crystals", Zeit. f. Phys. B, (1992).

16. A. Chang, Z. Y. Rong, Yu. M. Ivanchenko, F. Lu, and E. L. Wolf " Observation of Large Tunneling-Conductance Variations in Direct Mapping of the Energy Gap on Single Crystal $Bi_2Sr_2CaCu_2O_8$", Phys. Rev. B 46 5692 (1992).

17. (P) Yu. M. Ivanchenko, "Microwave Absorption in High-T_c Superconductors", Phys. Rev. Lett. (Submitted).

18. K. K. Likharev and V. K. Semenov, "RSFQ Logic/Memory Family: A New Josephson-Junction Technology for Sub-Terahertz-Clock-Frequency Digital Systems", IEEE Trans. Appl. Superc. 1 3, (1992).

19. (P) Yu. M. Ivanchenko, " Vortex Ring Excitations in Layered Superconductors", Phys. Rev. Lett. (submitted).

20. S. Martin, A. T. Fiory, R. M. Fleming, G. P. Espinosa, and A. S. Cooper, "Vortex-Pair Excitation Near the Superconducting Transition of $Bi_2Sr_2CaCu_2O_8$ Crystals", Phys. Rev. Lett. 62 677 (1989).

21. L. N. Bulaevskii, M. Ledvij, and V. G. Kogan, "Fluctuations of Vortices in Layered High-T_c Superconductors", Phys. Rev. Lett. 68 3773 (1992).

Phys. Rev. Lett. (subm.)

APPENDIX A

Microwave Absorption in High-T_c Superconductors*

Yu. M. Ivanchenko

Department of Physics, Polytechnic University
Six MetroTech Center, Brooklyn, NY 11201

Abstract

It is shown that the model describing a High-T_c superconductor (S) as a layered structure with Josephson coupling between S-layers should lead to appearance of substantial low frequency losses in the vicinity of T_c. These losses are caused by the interaction of supercurrents with fluctuating magnetization usually introduced by the copper ions.

PACS numbers: 74.20.-z, 74.30.Gn, 74.70.Vy

*Work supported by Air Force Office of Scientific Research, Grant AFOSR-89-0338.

Soon after the discovery of the anisotropic high-T_c superconductors an unusually strong low frequency absorption was found in these new materials (see Refs. [1-6]). A theoretical explanation for this phenomenon was given on the basis of flux motion in an effective Josephson medium (see for instance [7]). In this letter we show that there is an intrinsic mechanism related to the particular nature of high-T_c materials which also leads to such a phenomenon.

At present no one doubts, that the layered structure contributes essentially to the observed properties of such superconductors. On the other hand, practically all high-T_c superconductors, under the proper variation of the oxygen content regulating the carrier concentration, become magnetically ordered materials. There is also a region on the phase diagram where coexistence of the magnetism with the superconductivity is possible. The latter may mean that, even in the region of strong superconductivity, interaction between superconducting degrees of freedom and local or quasilocal magnetic moments could affect not only the thermodynamic, but also electrodynamic properties of such superconductors. Here we show, on an example of a simple model, how such interactions affect electrodynamics, leading to a temperature-dependent low frequency absorption. As the layered structure of the high-T_c oxides is often imitated by Josephson coupled regions of strong superconductivity, let us consider a Josephson junction with an insulating layer with width $2d$. This layer is assumed to be a magnetically ordered material at temperatures lower than the critical temperature T_m ($T_c > T_m$) in the absence of superconducting electrodes.The free energy for such a system can be written as

$$\mathcal{F} = \int d^2\boldsymbol{r} \left\{ \epsilon \left[\frac{(\nabla\phi)^2}{2} + \frac{1-\cos\phi}{\lambda_j^2} \right] - \right.$$
$$\left. - \nu \left[\boldsymbol{M}\boldsymbol{n}\right] \nabla\phi + \frac{\kappa}{2} \left[\frac{\tau_m \boldsymbol{M}^2}{\xi^2} + (\nabla \boldsymbol{M})^2 \right] \right\}, \tag{1}$$

where ϕ is the phase difference, λ_j is the Josephson penetration length, $\epsilon = \Phi_0^2/(4\pi)^2\pi\Lambda$, Λ is the region of magnetic field penetration ($\Lambda = 2(\lambda_L + d)$), Φ_0 is the magnetic flux quantum, $\nu = d\hbar c/e\Lambda$, $\boldsymbol{n}$ is a unit vector in the direction of tunneling (z-direction), the constant κ will be estimated below, $\tau_m = (T - T_m)/T_m > 0$ and ξ is a value of the magnetic, low temperature correlation length. In Eq. 1 the term proportional to ν is the energy of interaction between moments and magnetic fields caused by superconducting currents in the junctions. We have also omitted higher order terms with respect to M, as the consideration here is restricted only to a positive value of τ_m . Let us suppose that the critical temperatures T_c and T_m are distinctly different. In such a case, the equilibrium phase difference in the vicinity of T_c is equal to zero, as well as $M = 0$. Nonetheless, with the decrease of τ_m at some temperature, it is possible to make the free energy lower than zero owing to the interaction of the magnetic moments with the currents in the system. Such a state will be an essentially nonhomogeneous state with ϕ varying in space. In order to find the value of the temperature $\tau_{m1} > 0$ for such a transition, one has to study the spectrum of excitations for the free energy Eq. 1. After the expansion of the cosine in the integral and diagonalizing of the Gaussian form, one can find the following two branches $\epsilon_\pm$ of excitations

$$\epsilon_\pm(k) = \frac{\epsilon_m(k) + \epsilon_j(k)}{2} \pm \sqrt{\left(\frac{\epsilon_m(k) - \epsilon_j(k)}{2}\right)^2 + \bar{\nu}^2 k^2}. \qquad (2)$$

Here $\epsilon_m(k) = \epsilon_0(k^2 + \xi^{-2}\tau_m)$ is the energy of magnetic excitations in the absence of interactions, $\epsilon_j = \epsilon(k^2 + \lambda_j^{-2})$ is the energy of the Josephson phase fluctuations, $\bar{\nu} = \nu\mu_b/\Omega$, where Ω is the volume corresponding to the value of magnetization equal to the Bohr magneton μ_b of the layer in the ordered state, and the energy $\epsilon_0 = \kappa\mu_b^2/\Omega^2 \approx 2d\xi^2 T_m/\Omega$. In this problem we introduce the dimensionless parameters $y = (\epsilon_0/\epsilon)^{1/2}$, $\delta = \xi/\lambda_j$, and $\beta = \bar{\nu}\xi/\sqrt{\epsilon_0\epsilon}$. Typical values of these parameters for high-T_c superconductors can be estimated as follows. The values Λ and λ_j are of the order of λ_c and λ_{ab} (see for instance [8]), the correlation length $\xi \sim 10\mathring{A}$, the value $\Omega^{1/3}$ ranges from $1\mathring{A}$ to $10\mathring{A}$, T_m can be of the order of T_c or lower. These values give the following estimates $y \sim 10^{-1} \div 10$, $\delta \sim 10^{-2}$, and $\beta \sim 0.3 \div 10^{-2}$. The ratio $\epsilon_m(0)/\epsilon_j(0) \approx y^2\delta^{-2}$ is always large value. The latter means that the highest energy branch $\epsilon_+(k) \approx \epsilon_m(k)$, i.e. magnetic excitations are practically not affected by the fluctuations of the phase ϕ. On the contrary, phase fluctuations can be essentially affected by the presence of magnetic degrees of freedom. In Fig. 1 the dependence of ϵ_k is shown at different τ_m. As one can see from Eq. 2 at $\tau_m = \tau_0 \equiv \beta^2 - \delta^2$ the value $\epsilon_-(k) - \epsilon_j(0) \propto k^4$ at small k. When $\tau_m < \tau_0$, $\epsilon_-(k) - \epsilon_j(0) \propto -k^2$ at small k and it reaches minimum at $k^2 = k_{min}^2 \equiv \xi^2(\beta^2 - \tau_m - \delta^2)/2$. The function $\epsilon_-(k)$ touches the horizontal axis at the temperature $\tau_m = \tau_{m1} \equiv (\beta - \delta)^2$ at $k_{min}^2 = \xi^{-2}\delta(\beta - \delta)$.

Below this temperature there is no homogeneous solution of the equations

$$\frac{\delta\mathcal{F}}{\delta\phi(\boldsymbol{r})} = \epsilon\left(-\boldsymbol{\nabla}^2\phi + \frac{\sin\phi}{\lambda_j^2}\right) + \nu\mathrm{Div}\,[\boldsymbol{M}\boldsymbol{n}] = 0 \tag{3}$$

and

$$\frac{\delta\mathcal{F}}{\delta\boldsymbol{M}(\boldsymbol{r})} = \kappa(\xi^{-2}\tau_m - \boldsymbol{\nabla}^2)\boldsymbol{M} - \nu[\boldsymbol{n}\boldsymbol{\nabla}\phi] = 0, \tag{4}$$

with $\phi = 0$ and $\boldsymbol{M} = 0$, as the system at these values of ϕ and $\boldsymbol{M}$ is thermodynamically unstable. Therefore, at the temperature $\tau_m = \tau_{m1}$ the system undergoes a transition to a nonhomogeneous state characterized by the presence of supercurrents and two-dimensional (in the limit $d \to 0$) magnetization in the layer. This state can be imagined as a periodic array of vortex loops enclosing cores, in which the magnetization reaches its maximum value.

Now, we are going to prove that additional losses must appear in the system resulting from the presence of the fluctuating magnetization. For this purpose let us evaluate the surface impedance ζ_{ik} of the system composed from successive superconducting (S) layers with the width $2D$ divided by nonsuperconducting (N) layers with the width $2d$. In the case of high-T_c materials magnetic moments introduced by copper ions are usually positioned in the superconducting layers. Nonetheless, the magnetization inside the layer is screened and related to the surface of these layers. Therefore, we can describe the N-layer by the model with the free energy of Eq. 1. In such a system the surface impedance is strongly anisotropic. In the case when the material occupies the half space $y \leq 0$, with the layers parallel to the x-axis the $\zeta_{xx} \equiv \zeta_a$ component of the impedance can be measured when in electric and magnetic fields only E_x and H_z are not equal to zero. The impedance should be defined as (see for instance [9]) $\zeta_a = 4\pi\overline{E}_x/\overline{H}_z c$ where the overline means averaging of the field on the scale $2(d + D)$ along the z-direction. Considering $E_x, H_z \sim \exp i(ky - \omega t)$ and using Maxwell's equations, one can reduce the ζ_a component of impedance to

$$\zeta_a = \frac{4\pi}{c^2}\frac{\omega}{k(\omega)}, \tag{5}$$

where the equation defining the function $k(\omega)$ can be obtained from the continuity of E_x on the $S - N$ boundaries as

$$k^2 = \frac{4\pi i\omega}{c^2}\left[\sigma_N(k,\omega)(1-\rho) + \sigma_S(\omega)\rho\right], \tag{6}$$

where $\rho = D/(D+d)$. In this equation we introduce complex conductivities as characteristics of N and S layers. The value σ_S has the standard definition $\sigma_S(\omega) = \sigma_n + ic^2/4\pi\omega\lambda_L^2$, the value σ_N is defined below.

The component $\zeta_{zz} \equiv \zeta_c$ can be measured when E_z and H_x are not equal to zero as $\zeta_c = 4\pi\overline{E}_z/\overline{H}_x c$ leading to the same formal definition as given by Eq. 5. However in this case, continuity of H_x leads to the following equation defining the function $k(\omega)$

$$k^2 = \frac{4\pi i\omega}{c^2}\frac{1}{\sigma_N^{-1}(k,\omega)(1-\rho)+\sigma_S^{-1}(\omega)\rho}. \tag{7}$$

From Eqs. 6 and 7 one can see that when $|\sigma_S(\omega)| \gg |\sigma_N(k,\omega)|$ (which should be the case if σ_N is defined by the Josephson-like coupling between S layers), the value ζ_a is practically defined by large shunting currents flowing in the superconducting parts of the material. On the contrary, ζ_c is governed by N layers which, in the presence of magnetic moments interacting with currents, has σ_N essentially dependent on k. In order to estimate the function $\sigma_N(k,\omega)$, we need to generalize Eqs. 3 and 4 for the case of a time dependent perturbation and use the linearized version of the equations

$$\Gamma_\phi \frac{\partial\phi(\boldsymbol{r})}{\partial t} = -\frac{\delta\mathcal{F}}{\delta\phi(\boldsymbol{r})} \tag{8}$$

and

$$\Gamma_m \frac{\partial M(\boldsymbol{r})}{\partial t} = -\frac{\delta\mathcal{F}}{\delta M(\boldsymbol{r})}, \tag{9}$$

where the coefficients $\Gamma_{\phi,m}$ are different owing to the difference in the relaxation of currents and magnetic moments. The coefficient Γ_ϕ can be expressed through the quasiparticle tunneling conductance σ_T as $\Gamma_\phi = 2\Phi_0^2\sigma_T/(4\pi)^2dc^2$. Using Eqs. 8, 9, and the Josephson relation $\partial\phi(\boldsymbol{r},t)/\partial t = 4edE_z(\boldsymbol{r},t)/\hbar$ one can obtain the following expression

$$\sigma_N(k,\omega) = \sigma_T + \frac{ic^2\tau}{4\pi\omega\lambda_e^2} - \frac{ic^2}{4\pi\omega}\frac{(1-\rho)k^2\beta^2\xi_0^{-2}}{-i\omega\gamma_m + k^2 + \xi_0^{-2}(\Delta\tau - \tau)}, \tag{10}$$

where we have taken into account that $\Lambda = 2(\lambda_L \tanh D/\lambda_L + d) \approx 2(D+d)$ and have used approximations for material characteristics as $j_c(\tau) = j_c(0)\tau$ and $\lambda_L = \lambda_L(0)\tau^{-1/2}$ applicable when $\tau = (T_c - T)/T_c \ll 1$. We also introduced in Eq. 10 notations $\lambda_e = \lambda_j(0)(\lambda_L(0)/(D+d))^{1/2}$, $\gamma_m = \Gamma_m/\kappa$,

$\xi_0^{-2} = \xi^{-2}T_c/T_m$, and $\Delta\tau = (T_c - T_m)/T_c$. Using Eqs. 10 and 7 one can calculate the surface impedance ζ_c as a function of temperature and other physical parameters. The results of such calculations are shown in Fig.2 and Fig.3 for the case $\sigma_T \ll \sigma_n$. The ratio σ_T/σ_n can be estimated from d.c. measurements of resistivity in normal state as ρ_{ab}/ρ_c. This ratio may substantially vary depending on oxygen content, type of impurities, and their concentrations. For $Bi_2Sr_2CaCu_2O_x$, according to [10], ρ_{ab}/ρ_c is of the order of 10^{-4}. In Fig.2a, one can see that the temperature dependence of real and imaginary parts ζ_c in very close vicinity of T_c, resembles behavior in a traditional superconductor. When τ approaches τ_1 an essential difference appears. The real part increases reaching maximum at $\tau \approx \tau_1$, while $Im\zeta_c$ may turn to zero. Thus the reaction of a sample may be practically active instead of the usual overwhelming inductive part. The behavior of ζ_c can only be extrapolated in the region $\tau < \tau_1$ under the assumption that the structure arising at $\tau = \tau_1$ is pinned. Otherwise below τ_1 one may expect even increase of $Re\zeta_c$ in some range of temperatures. The tendency to increase of losses is especially well seen in Fig.2b, where one can see transformation of $Re\zeta_c$ with frequency. In the range of frequencies $\omega/\omega_0 \ll 1$ (where $\omega_0 = c^2/4\pi\sigma_T\lambda_e^2$) the real part undergoes substantial changes so that losses in the superconducting state may be even higher then in the normal state, as a consequence of the interaction of supercurrents with the fluctuating magnetization. The characteristic frequency ω_0 can be estimated for the case of $BiSrCaCuO$ systems being of the order of 10^9 Hz. Influence of other parameters (δ and β) is shown in Fig.3. These two parameters affect the value τ_1 as well as the level of losses. The influence of the magnetic relaxation parameter γ_m is not essential so far as $x = \gamma_m c^2(1-\rho)/4\pi\sigma_T \leq 1$. In the case of large x all curves will be smoothened.

In conclusion, we think that experimental study of low-frequency losses in single crystals can give useful information on the interaction of magnetic and superconducting collective excitations in high-T_c materials. Especially informative should be experiments in which losses are studied along with change of the oxygen content and (or) variations of host ions affecting magnetic moments of copper ions.

I am grateful to Prof. E. L. Wolf for interesting discussion of this work. This work was supported by Air Force Office of Scientific Research, Grant AFOSR-89-0338.

References

[1] R. Durny, J. Hautala, S. Ducharme, B. Lee, O. G. Symko, P. C. Taylor, D. J. Zheng, and J. A. Xu, Phys. Rev. B **36**, 2361, (1987).

[2] K. W. Blazey, K. A. Muller, F. G. Bednorz, W. Berlinger, G. Amoretti, E. Buluggiu, A. Vera, and F. C. Matacotta, Phys. Rev. B **36**, 7241, (1987).

[3] K. A. Muller, M. Takashige, and J.G. Bednorz, Phys. Rev. Lett. **58**,1143, (1987).

[4] K. Khachaturyan, E. R. Weber, P. Tejedor, A. M. Stacy, and A. M. Portis, Phys. Rev. B **36**, 8309, (1987).

[5] E. J. Pakulis and T. Osada, Phys. Rev. B **37**, 5940, (1988).

[6] W. J. Tomasch, H. A. Blackstead, S. T. Ruggiero, P. J. McGinn, J. R. Clem, K. Shen, J. W. Weber, and D. Boyne, Phys. Rev. B **37**, 9864, (1988).

[7] E. B. Sonin and A. K. Tagantsev, Phys. Lett. A **140**, 127, (1989).

[8] B. Batlogg, Phys. Today **44**, 44 (1991).

[9] L. D. Landau and E. M. Lifshits, *Electrodynamics of Solids,* Science, Moscow, (1982).

[10] X. D. Xiang, W. A. Vareka, A. Zettl, J. L. Corkill, M. L. Cohen, N. Kijima, and R. Gronsky, Phys. Rev. Lett. **68**, 530, (1992).

FIGURE CAPTIONS

Fig.1 Transformation of the lowest (phase fluctuations) branch of collective quasiparticle excitations with temperature (see Eq. 2) Parameters are equal to: $\beta^2 = 10^{-1}$, $\delta^2 = 5 \times 10^{-2}$, $10\tau_m = 2;\ 1.5;\ 0.6;\ 0.4;\ 0.2;\ 0.087$ ($\tau_{m1} \approx 8.7 \times 10^{-3}$).

Fig.2 Dependence of real (a, b) and imaginary (a) parts of the surface impedance ζ_c on temperature. $R_\square$ is real part of surface impedance at $T = T_c$. Parameters are equal to: $\Delta\tau = 7 \times 10^{-2}$, $x = 0.1$.

(a) $\beta^2 = 2 \times 10^{-2}$, $\delta^2 = 10^{-2}$, $\omega_0/\omega = 10^2$.

(b) $\beta^2 = 5 \times 10^{-2}$, $\delta^2 = 5 \times 10^{-2}$, $\omega_0/\omega = 2;\ 10;\ 10^2;\ 10^3;\ 10^4$.

Fig.3 Variation of the temperature dependence of $Re\zeta_c$ with the change of parameters β and δ. Parameters are equal to: $\Delta\tau = 7 \times 10^{-2}$, $x = 0.1$, $\omega_0/\omega = 10^2$.

(a) $\delta^2 = 10^{-2};\ 2 \times 10^{-2};\ 3 \times 10^{-2};\ 5 \times 10^{-2};\ 7 \times 10^{-2};\ 0.1;\ 0.15;\ 0.2,\ 5 \times 10^{-2}$.

(b) $\delta^2 = 10^{-2}$, $\beta^2 = 2 \times 10^{-2};\ 3 \times 10^{-2};\ 4 \times 10^{-2};\ 5 \times 10^{-2};\ 6 \times 10^{-2}$.

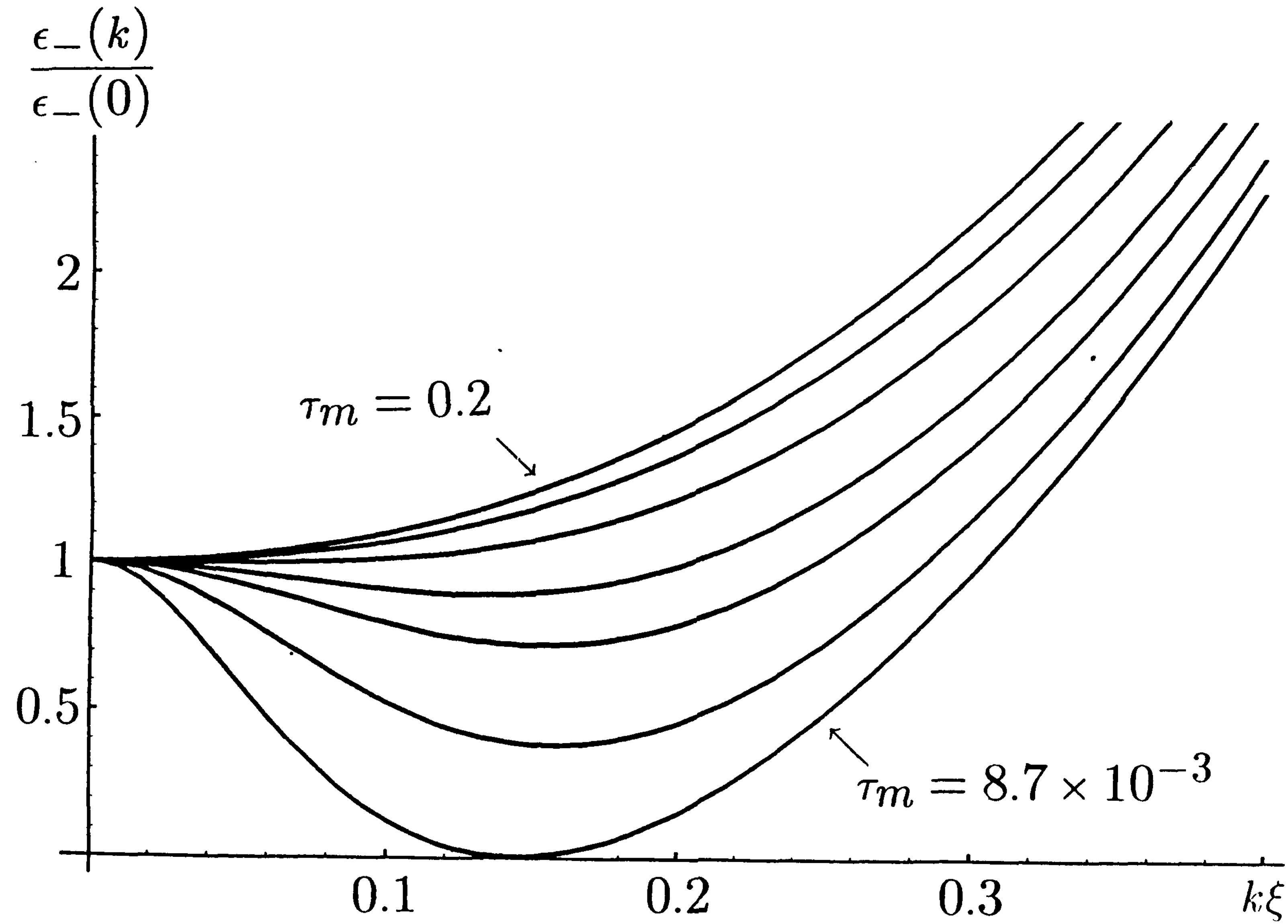

$\frac{\epsilon_-(k)}{\epsilon_-(0)}$
2
1.5
1
0.5
$\tau m = 0.2$
$\tau m = 8.7 \times 10^{-3}$
0.1
0.2
0.3
$k\xi$

Fig. 1

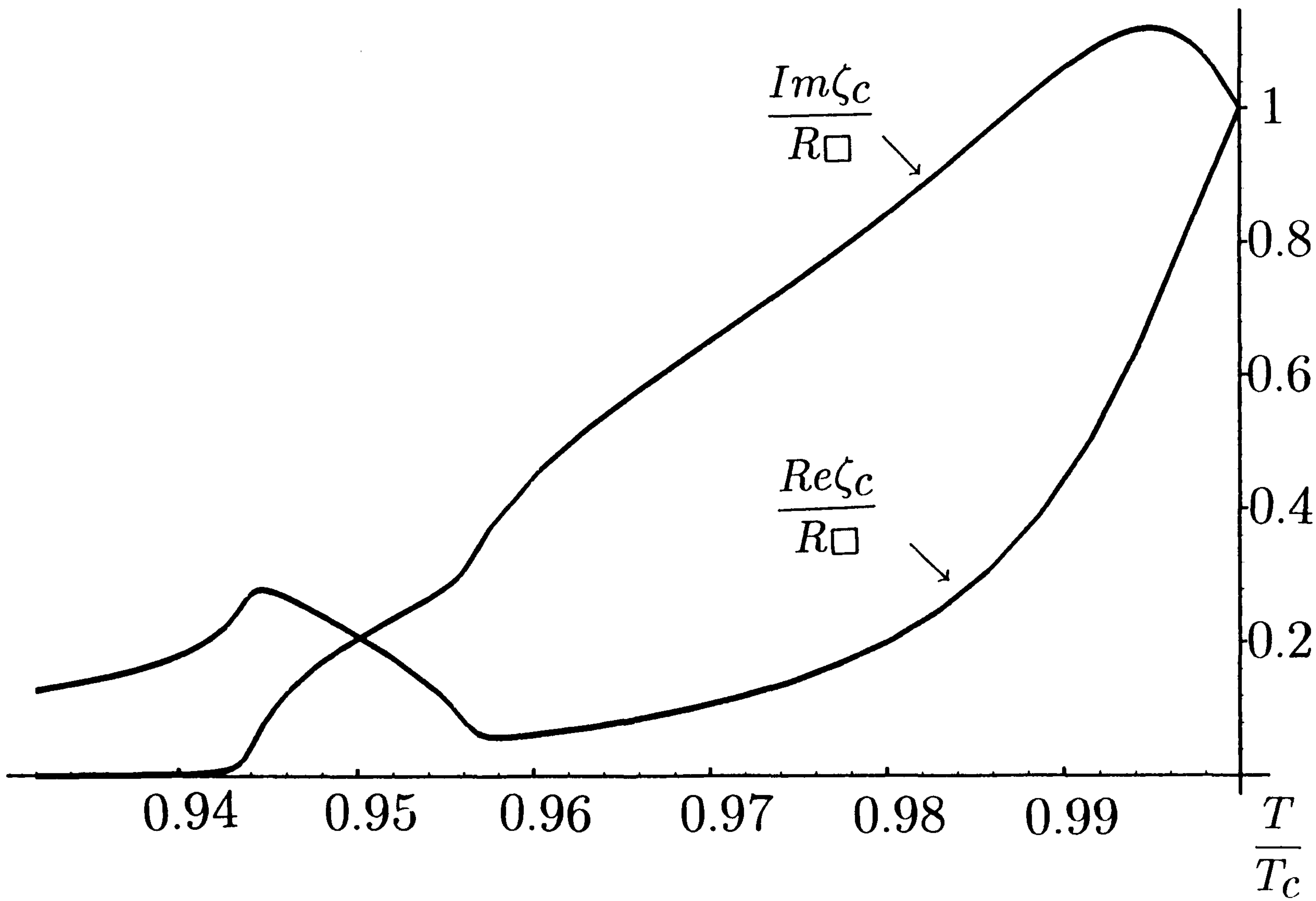
$\frac{Im\zeta_c}{R_\square}$
$\frac{Re\zeta_c}{R_\square}$
1
0.8
0.6
0.4
0.2
0.94
0.95
0.96
0.97
0.98
0.99
$\frac{T}{T_c}$

Fig 2(a)

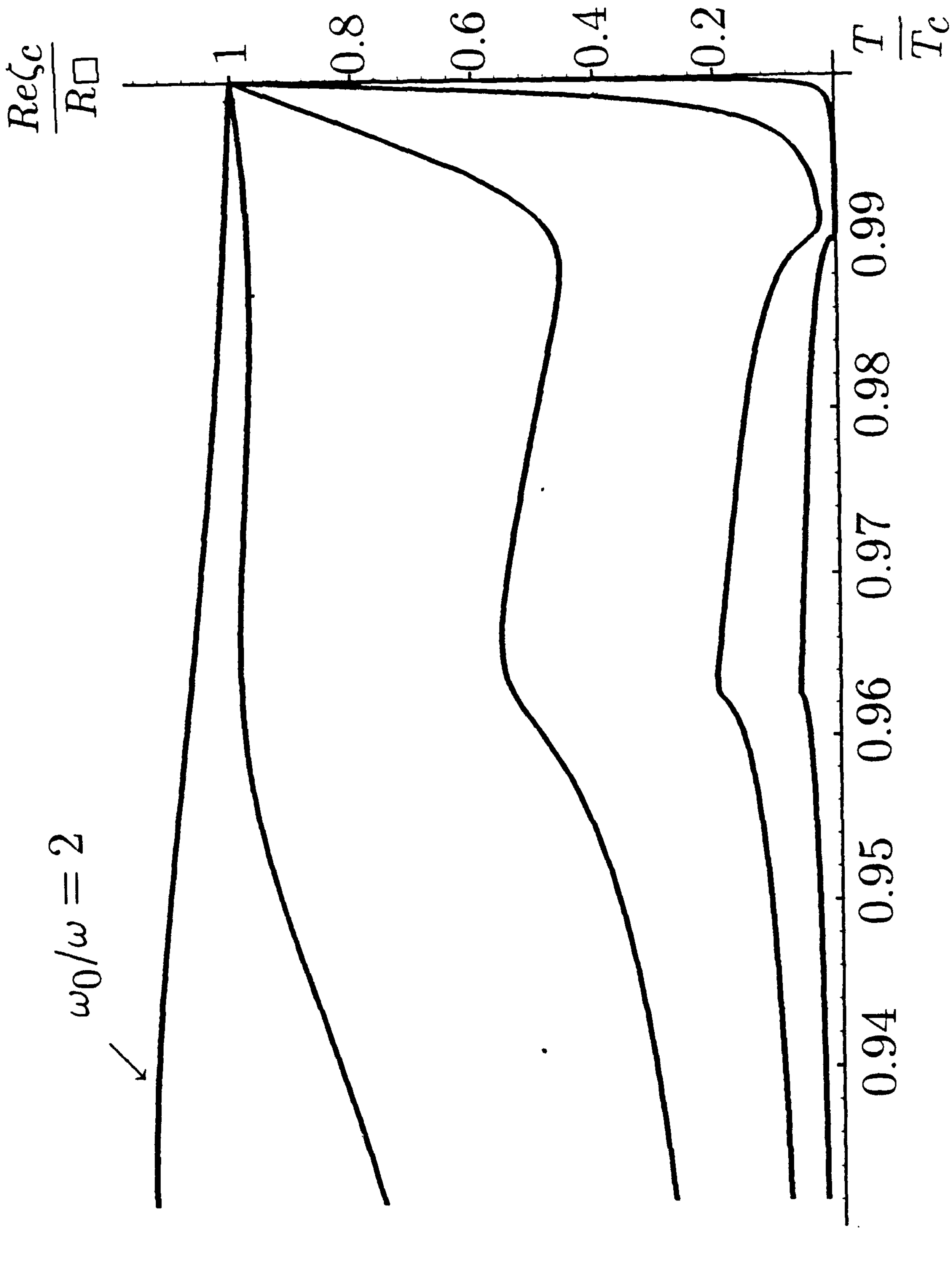

$\frac{Re\zeta c}{R\square}$
1
0.8
0.6
0.4
0.2
$\frac{T}{T_c}$
0.99
0.98
0.97
0.96
0.95
0.94
$\omega_0/\omega = 2$

Fig. 2(b)

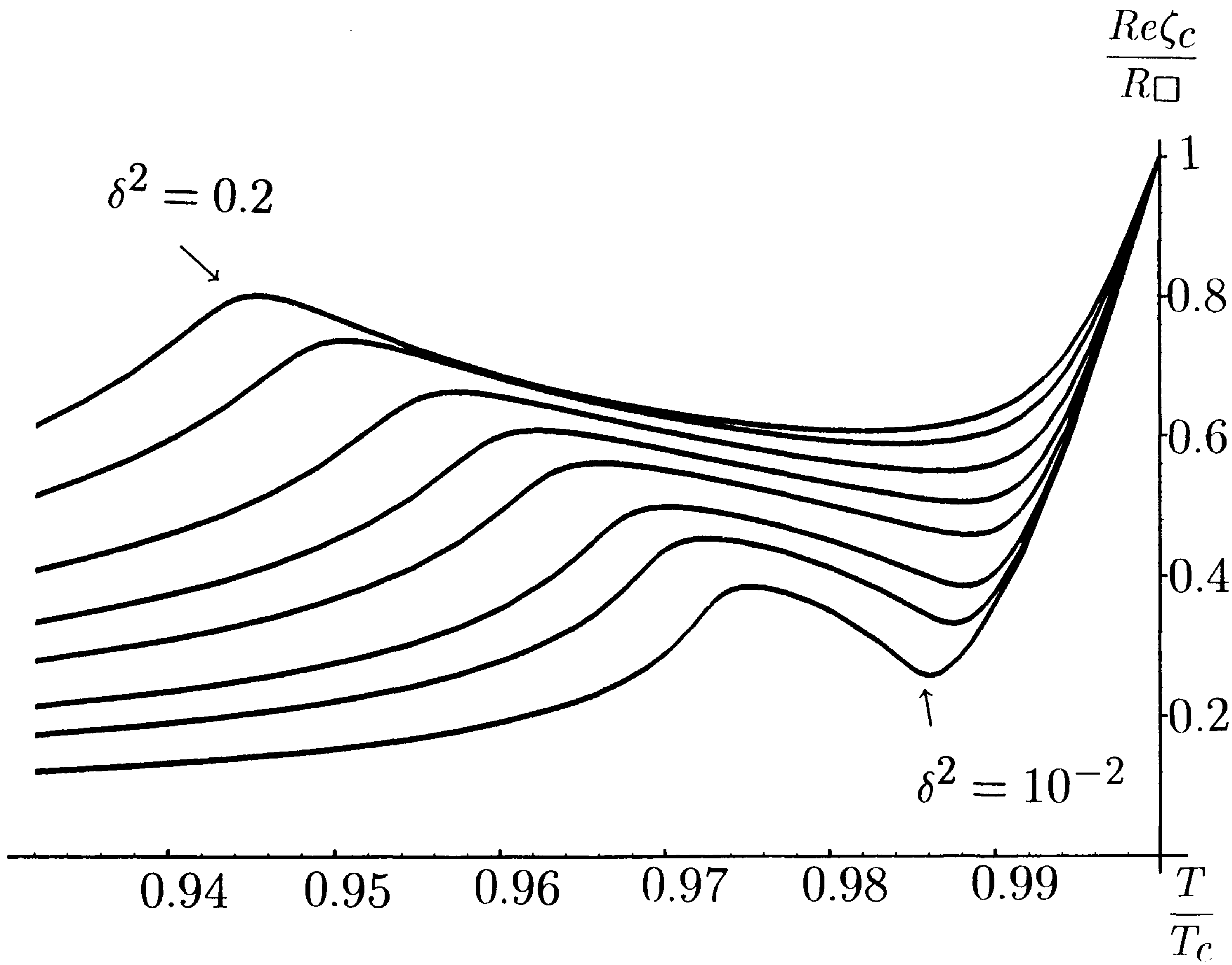
$\frac{Re\zeta_c}{R_\square}$
1
0.8
0.6
0.4
0.2
$\delta^2 = 0.2$
$\delta^2 = 10^{-2}$
0.94
0.95
0.96
0.97
0.98
0.99
$\frac{T}{T_c}$

Fig 3 (a)

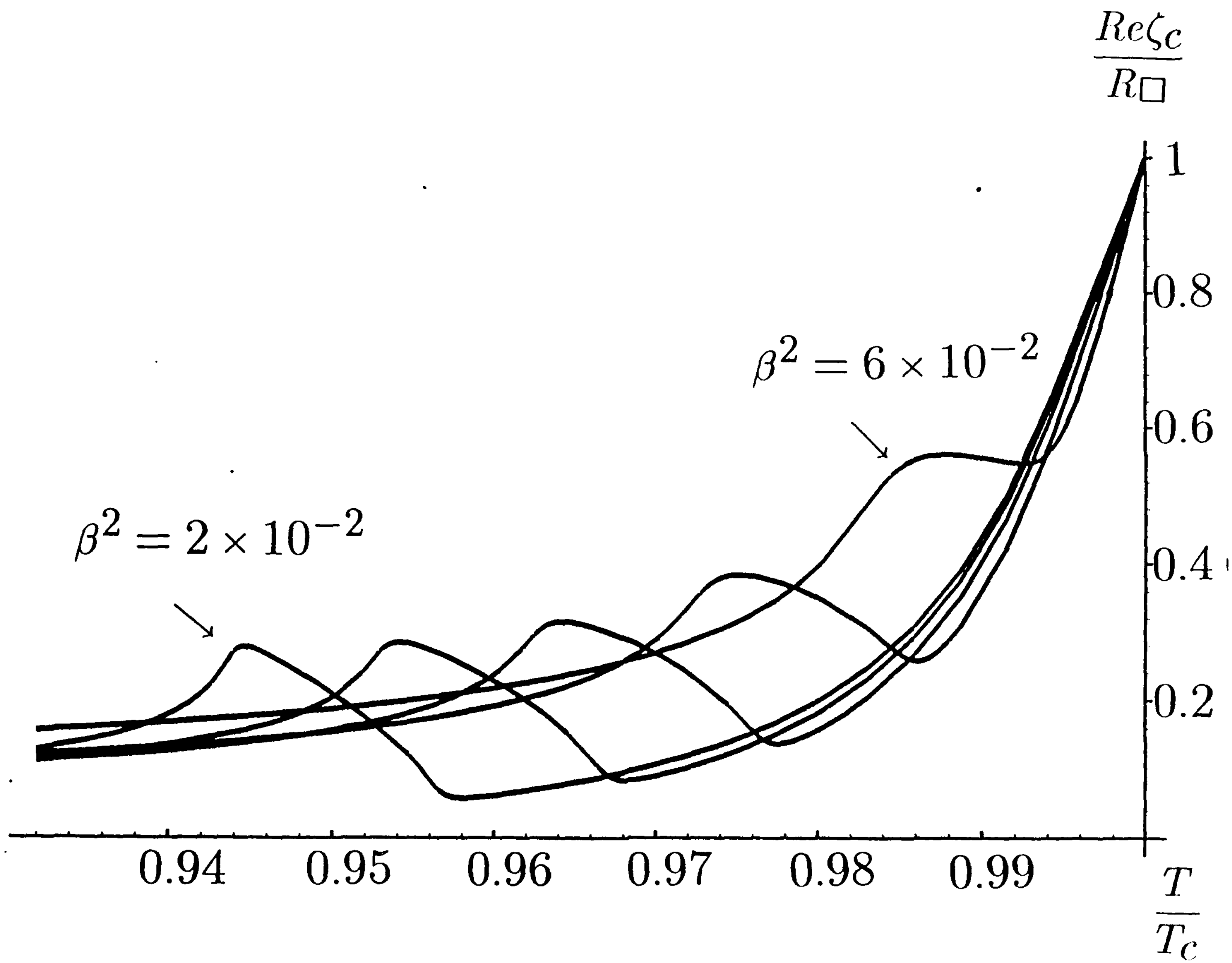

$\frac{Re\zeta_c}{R_\square}$
1
0.8
0.6
0.4
0.2
$\beta^2 = 6 \times 10^{-2}$
$\beta^2 = 2 \times 10^{-2}$
0.94
0.95
0.96
0.97
0.98
0.99
$\frac{T}{T_c}$

Fig 3(b)

APPENDIX B Phys. Rev. Lett. (subm).

Vortex Ring Excitations in Layered Superconductors*

Yu. M. Ivanchenko

Department of Physics, Polytechnic University
Six MetroTech Center, Brooklyn, NY 11201

Abstract

It is shown that, in a periodic array of two different superconducting layers, a special kind of thermal excitations can be found in the vicinity of T_c. These excitations are vortex rings positioned in the layer with weaker superconductivity. For parameters corresponding to high-T_c superconductors these excitations are most likely to consist of two coupled vortex rings with opposite helicities, separated by the layer with stronger superconductivity. Such a kind of excitations under the decrease of temperature are pinned and contribute to randomization of the superconducting state at low temperatures. Estimates are made for the relative value of density of states within the gap region and characteristic length of the random structure caused by the double ring excitations.

PACS numbers: 74.20.De, 74.70.Jm, 74.70.Vy

*Work supported by Air Force Office of Scientific Research under Grant AFOSR-89-0338 and US Department of Energy, Office of Basic Energy Sciences, under Grant DE-EG02-87ER45301.

It is now widely recognized that thermal excitations of $2D$-vortices play an important role in the magnetic and transport properties of anisotropic layered superconductors (SC). This phenomenon substantially influences extremely anisotropic systems like Bi- or Tl-based high-T_c oxides or artificial superconducting superlattices. A conventional model describing such compounds was first advanced by Lawrence and Doniach [1]. This model deals with a periodic array of SC-layers coupled by weak Josephson links. In Ref.[2] a squeezed vortex in a similar structure has been considered as a constituent for pairs leading to Berezinsky-Kosterlitz-Thouless transition [3], [4]. A pair of vortices in a layered superconducting structure can be imagined as a single vortex loop with the normal core forming something close to a rectangle, which small sizes are inside the film with stronger superconductivity. Here we consider a ring shaped loop, Which is completely confined to the weaker layer. Such rings cannot directly contribute to the 2D-like behavior. Nonetheless, as it is shown, they may essentially affect superconducting properties of layered structures. In the following we consider a simplified model for a strict mathematical description of a ring. We assume that a cell of a layered structure consists of two layers with the thicknesses $2d_1$ and $2d_2$. Each layer is a London superconductor characterized by the bulk field penetration length λ_1 or λ_2. These layers alternatively form a periodic structure in z-direction. The magnetic field distribution can be found as a solution of the London equation which for this case takes the form (see [5])

$$\boldsymbol{h}(\boldsymbol{r}) + \nabla \times \left\{\lambda^2(z) \nabla \times \boldsymbol{h}(\boldsymbol{r})\right\} = \Phi_0 \oint dl \delta(\boldsymbol{r} - \boldsymbol{l}), \tag{1}$$

where Φ_0 is the magnetic flux quantum and the integration should be carried out along the curve of the ring with the length $L = 2\pi\rho$. This equation must be completed by the boundary conditions reflecting the continuity of the magnetic field and the normal component of current. We also assume that the ring is positioned at $\boldsymbol{r}_\perp = 0$ in the middle of the layer (plane $z = 0$,) with the penetration length λ_1, which is the largest of all characteristic lengths λ_2, d_1, and d_2. For such a configuration the magnetic field possesses a radial symmetry and can be represented by $\boldsymbol{h} = \boldsymbol{\tau} h(r, z)$, where $\boldsymbol{\tau}$ is the azimuthal unit vector. The value h satisfies the following equations hold in the layers

$$\left\{\frac{1}{\lambda_k^2} + \frac{1}{r^2} - \frac{\partial^2}{\partial r^2} - \frac{1}{r}\frac{\partial}{\partial r} - \frac{\partial^2}{\partial z^2}\right\} h_{n_k}(r, z) = \delta_{n_k,0} \frac{\Phi_0}{\lambda_1^2} \delta(r - \rho)\delta(z), \tag{2}$$

where n_k $(k = 1,2)$ are integers numbering layers, $n_k = 2p$ for the layers with the penetration length λ_1. The boundary conditions for Eqs. 2 can be written as

$$\begin{aligned} h^+_{2p}(r) &= h^-_{2p+1}(r), & h^+_{2p+1}(r) &= h^-_{2(p+1)}(r), \\ \lambda_1^2 h^+_{2p,z}(r) &= \lambda_2^2 h^-_{2p+1,z}(r), & \lambda_2^2 h^+_{2p+1,z}(r) &= \lambda_1^2 h^-_{2(p+1),z}(r), \end{aligned} \tag{3}$$

where $h^\pm$ denote upper $(+)$ and lower$(-)$ boundary of a layer, h_z is a derivative with respect to z. In the following we assume that $\lambda_1 \gg \lambda_2$. This assumption essentially simplifies calculations and corresponds to the real physical situation, especially if one would apply this consideration to the case of high-T_c materials. When λ_1 essentially exceeds all other characteristic lengths the set, Eqs. 2 with the boundary conditions Eq. 3, allows to apply the separation of variables. For this purpose, let us average the equation for the first layer from the set of Eqs. 2 over the thickness. After that the solutions of Eqs. 2 can be represented as $h_n(r,z) = h(r/\lambda_\perp)Z_n(z/\lambda_\perp)$, where, if one scales all lengths r, ρ and z in the units of $\lambda_\perp$, the function $h(r)$ is defined by

$$h(r) = \Phi\left\{\Theta(r-\rho)I_1(\rho)K_1(r) + \Theta(\rho - r)K_1(\rho)I_1(r)\right\}, \tag{4}$$

where I_1 and K_1 are Bessel's functions of imaginary argument. In this equation the scaling factor $\lambda_\perp$ must be defined from the solvability condition for the whole set. Strictly speaking, the Heaviside's step function $\Theta(r)$ in Eq. 4 can be written only approximately and in the vicinity $|r-\rho| \propto d_1/\lambda_\perp, d_2/\lambda_\perp$ they should be replaced by a smooth function which can be obtained from an exact solution (which is very cumbersome). In the following, corrections from such a replacement would give a value of the order of $(d_i/\lambda_\perp)^2$ which, in the accepted here approximation, is a very small value. The quantity Φ in Eq. 4 is defined as $\Phi = \Phi_0\lambda_\perp/2\lambda_1^2 d_1$. This definition gives the boundary conditions at the lower layer $Z_1^- = 1$ and $Z_{1,z}^- = d_1\chi_1^2\lambda_1^2/\lambda_\perp\lambda_2^2$. The functions Z_n satisfy homogeneous equations $Z_{n,zz} - \chi_n^2 Z_n = 0$, with $\chi_{n_k}^2 = (\lambda_\perp/\lambda_k)^2 - 1$. The solutions of these equations can be represented in the form

$$Z_n = A_n^+ e^{\chi_n(z-z_n)} + A_n^- e^{-\chi_n(z-z_n)}, \tag{5}$$

where $z_n = n(d_1+d_2)/\lambda_\perp$, i.e. z_n is positioned in the middle of the n-th layer. With the use of Eq. 5 one can rewrite the set of boundary conditions Eqs. 3

in the matrix form $L_1^+ A_{2p} = L_2^- A_{2p+1}$ and $L_2^+ A_{2p+1} = L_1^- A_{2(p+1)}$, where the following matrices are introduced

$$L_k^\pm = \begin{pmatrix} 1 & 1 \\ y_k & -y_k \end{pmatrix} \exp(\pm\sigma x_k), \quad \sigma = \begin{pmatrix} 1 & 0 \\ 0 & -1 \end{pmatrix},$$
$$A_n = \begin{pmatrix} A_n^+ \\ A_n^- \end{pmatrix}, \; A_1 = \frac{e^{\sigma x_2}}{2} \begin{pmatrix} 1 + x_1 y_1/y_2 \\ 1 - x_1 y_1/y_2 \end{pmatrix}, \quad \begin{matrix} y_k = \lambda_k^2 \chi_k / \lambda_\perp^2 \\ x_k = d_k \chi_k / \lambda_\perp \end{matrix} . \tag{6}$$

The solutions for the columns A_n can be written in the form $A_{2p} = (L_1^+)^{-1} N^p L_2^- A_1$ and $A_{2p+1} = (L_2^-)^{-1} N^p L_2^- A_1$, where the matrix N is defined as $N = P_1 P_2$ with

$$P_1 = \begin{pmatrix} \cos 2|x_1| & (\sin 2|x_1|)/|y_1| \\ -|y_1| \sin 2|x_1| & \cos 2|x_1| \end{pmatrix}, \quad P_2 = \begin{pmatrix} \cosh 2x_2 & (\sinh 2x_2)/y_2 \\ y_2 \sinh 2x_2 & \cosh 2x_2 \end{pmatrix}.. \tag{7}$$

As is seen from Eq. 7 the matrix N has $\det N = 1$ with two real and positive eigenvalues $(n_\pm)$ satisfying equality $n_+ n_- = 1$, i.e. $n_+ > 1 > n_-$. The amplitudes $A_n^\pm$ should decrease with the increase of n. Therefore, one must nullify terms increasing as n_+^p. Imposing this requirement one arrives at the following solvability condition

$$\frac{x_1}{y_1 y_2} + \frac{x_1 y_1}{y_2} \sqrt{1 + \left(\frac{x_1}{y_1 y_2}\right)} - 2\frac{x_1}{y_1 y_2} \coth 2x_2 = 0. \tag{8}$$

This equation defines the scaling parameter $\lambda_\perp$ which is the penetration length for perpendicular to the layers magnetic fields. Further simplification can be made when additional inequality holds $\lambda_2 \gg d_1 + d_2$. In this region of parameters on can get from Eq. 8 $\lambda_\perp = \lambda_1 \sqrt{d_1/\lambda_2}$. One can also obtain in this limit the effective penetration length for magnetic fields parallel to the layers $\lambda_\parallel = \lambda_2 (d_2 + d_1)/d_2$. The found solution for the magnetic field distribution helps to define energy of a vortex ring. The energy $E(\rho)$ can be expressed as an integral along the curve of the ring

$$E(\rho) = \frac{\Phi_0}{8\pi} \oint d\boldsymbol{l}\boldsymbol{h}(\boldsymbol{l}) \tag{9}$$

After carrying out the integration in Eq. 9 we arrive at

$$E(\rho) = \frac{\Phi_0 \Phi \lambda_\perp}{4} \rho^2 I_1(\rho) K_1(\rho) = E_0 \rho^2 I_1(\rho) K_1(\rho). \tag{10}$$

As one may expect, in the limit of large ρ ($\rho \gg 1$,) this energy can be written in a traditional form $E \approx \bar{H}_{c1}\Phi_0 L/4\pi$, where we have introduced the lowest first critical field in the layered structure equal to $\bar{H}_{c1} = \Phi_0/8\lambda_1\sqrt{d_1\lambda_2}$. When the external magnetic field is applied parallel to the layers, there are two "first critical" fields in such a structure. There is the lowest field $\bar{H}_{c1}$, when penetration of vortexes occur in the weak layer, and the field H_{c1} at which cores of vortexes enter into the layer characterized by λ_2. In the considered here limit $\bar{H}_{c1} \ll H_{c1}$. One can compare the energy Eq. 10 with the energy of a pair of oppositely directed squeezed vortexes $E_p(r)$ separated by the distance $r = (L - 2d_2)/2$ (see Ivanchenko *et al* [2]). In the same structure we always have $E < E_p$ at the same value of L. Nonetheless, the entropy contribution to the free energy of a pair makes its creation more favorable. The latter means that single vortex rings cannot essentially contribute to the $2D$-like behavior in the vicinity of the critical temperature. The energy of a ring excitation (RE) can be made essentially smaller if one considers a pair of vertex rings of opposite helicity separated by a layer with the strong superconductivity. The energy of such an excitation will be dependent on two radii ρ_1, ρ_2 and the separation distance R, and it can be calculated in the same manner. In this case instead of Eq. 9 we have

$$E(\rho_1, \rho_2, R) = \frac{\Phi_0}{8\pi}\left\{\oint_1 d\boldsymbol{l}\boldsymbol{h}_1(\boldsymbol{l}) + \oint_2 d\boldsymbol{l}\boldsymbol{h}_2(\boldsymbol{l}) + \oint_1 d\boldsymbol{l}\boldsymbol{h}_2(\boldsymbol{l}) + \oint_2 d\boldsymbol{l}\boldsymbol{h}_1(\boldsymbol{l})\right\}, \tag{11}$$

where the indices 1, 2 in integrals define integration paths along the first or the second ring, $\boldsymbol{h}_i$ is the field generated by the i-th ring. The smallest energy E_2 at a fixed vertex path length $L = 2\pi(\rho_1 + \rho_2)$ is realized when $\rho_1 = \rho_2 = L/4\pi = \rho$ and $R = 0$

$$E_2(\rho) = E(\rho, \rho, 0) = \frac{d_2\Phi_0^2}{4\lambda_2^2}\rho^2 I_1(\rho)K_1(\rho) = E_{20}\rho^2 I_1(\rho)K_1(\rho). \tag{12}$$

Now we will estimate an entropy contributions resulting from the liberty implied by the possible change of $\rho_1 = \rho + r/2$, $\rho_2 = \rho - r/2$, and R. In this case according to the general principles of statistical mechanics we have to define the free energy as

$$F = -T\ln\int dr\int dR\exp\left\{-\frac{E(\rho_1, \rho_2, R)}{T}\right\} = E_2(\rho) - T\ln f(\rho), \tag{13}$$

where the function $f(\rho) \propto \rho^{-1}$ when $E_{20}/T \gg 1$. The probability density $w(\rho)$ to find a double ring excitation (DRE) can be defined as $w(\rho) = Af(\rho)n(\rho)$, where A is a normalization constant and $n(\rho) = \exp[-E_2(\rho)/T]$ is a number of such excitations with the radius ρ. DRE can be thermally excited in the vicinity of T_c. In order to excite such an excitation one has to overcome a barrier with the energy E_b. In Fig.1 the dependence $E_2(\rho, z)$ on the separation of rings z is shown. This is a result of exact calculations which will be published elsewhere. The value of the lowest energy barrier can also be estimated with the help of Eq. 5 as $E_b(\rho)/E(\rho) \approx \lambda_1^2 d_1/\lambda_2^3 = \kappa$. This relation shows that the barrier energy can be more or less then the energy of an RE depending on the value κ. Let us estimate κ for $YBa_2Cu_3O_7$ as the most complete set of data is available for this material (see for instance [6]) $d_1 \approx 2d_2$, $2d_2 \approx 3.8\mathring{A}$, $\lambda_\perp = 1400\mathring{A}$, and $\lambda_{||} \approx 7000\mathring{A}$. From this data one can obtain $\lambda_1 \approx 3.5 \times 10^4\mathring{A}$, $\lambda_2 \approx 2.3 \times 10^3\mathring{A}$, and $\kappa \approx 0.3$. This shows that RE should not be as essential as DRE, because the latter have much lower energy ($E_2/E = 2d_2/\lambda_2 \approx 1.6 \times 10^{-3}$) and can be easily excited. DRE created at some temperature in the vicinity of T_c will be pinned with a decrease of temperature. Therefore, in the low temperature region should always be some finite density of pinned double vortex loops (DVL). The latter causes a finite density of quasiparticle states in the gap region. Such an effect is always seen in tunneling data. There has been advanced a number of explanations for the phenomenon (see as an example [7]). Let us estimate contribution of DVL into this density of states. We assume that along a vortex line in a layer some volume $V(\rho)$, equal to $2\pi^2\rho\lambda_\perp d_1^2$ is roughly in the normal state. Within the whole layer we have

$$\Delta V(\rho) = 2\pi^2\rho\lambda_\perp d_1^2 n(\rho)\Delta\Gamma(\rho), \tag{14}$$

where $\Delta\Gamma(\rho)$ is the volume of phase space corresponding to radii between $\rho + \delta\rho$ and ρ. This value can be estimated as follows. As DVL are created from the pinned DRE at some temperature T_p at which pinning occurs, we need to estimate $\Delta\Gamma$ for DRE at this temperature. We have an area ΔS on which the smallest cell is constituted by a ring with the area $S(\rho) = \pi\rho^2\lambda_\perp^2$. One should multiply $\Delta S/S(\rho)$ by the number of rings $m(\rho)$, which can be inserted into the area $S(\rho)$ without interaction between them, i.e. separated by the distance $\lambda_\perp$ along the radius $\rho\lambda_\perp$. This number is simply ρ (i.e. $m(\rho) = \rho\lambda_\perp/\lambda_\perp$). As a result, if one also takes into account that the smallest possible ring may have $\rho_{min} = d_1/\lambda_\perp$ the value $\Delta\Gamma$ can be estimated as

$$\Delta\Gamma(\rho) = \frac{\Delta S}{S(\rho)} m(\rho) \frac{\delta\rho\lambda_\perp}{d_1} = \frac{\Delta S \delta\rho}{\pi\rho\lambda_\perp d_1}, \tag{15}$$

Now the relative part $a_n = V_n/Sd_1$ of the normal volume can be estimated from Eq. 14 as

$$a_n \approx 2\pi \int_0^\infty d\rho e^{-\frac{E_2(\rho)}{T_p}} \approx \frac{\pi^{3/2}}{\gamma^{1/2}}, \tag{16}$$

where $\gamma = E_{20}(T_p)/2T_p$ is assumed to be much greater then unit. The formula Eq. 16 can be compared with the available experimental data. In the work [8] the density of states within the gap related to the normal density of states is approximately 0.25. This value should be compared with a_n. The value γ for $BiSrCaCuO$ crystals can be estimated as $10^2 - 10^3$ which gives quite reasonable agreement with this experiment. Additional experimental fact in favor of DVL also obtained in this work. One can estimate an average characteristic length l on which all superconducting properties should randomly vary due to the presence of DVL. This length is equal to

$$l = \lambda_\perp \langle \rho \rangle = \lambda_\perp \int_{\rho_{min}}^\infty d\rho\rho w(\rho) \approx \frac{\lambda_\perp}{\gamma^{1/2} |\ln \rho_{min}^2 \gamma|}. \tag{17}$$

This equation gives $l \approx 100\mathring{A}$ which is close to the value seen in [8]. One more qualitative fact found in [8] which agrees with the presence of DVL is: the regions on the surface of the crystal, with lower density of states in the gap, correspond to better superconductivity seen in the increase of density in the vicinity of the gap singularity.

In conclusion, we believe that DVL at low temperatures, originated from DRE existing in the vicinity of T_c, manifest themselves in additional randomization (in comparison with the normal state) of superconducting properties in high-T_c superconductors and layered structures. Most likely that such randomization has already been seen in experiment [8]. Further experiments which could contribute in clarification of this problem should compare levels of randomization in normal and superconducting states.

I am grateful to E. L. Wolf, fruitful discussions with whom, stimulated appearance of this work. This work was supported by Air Force Office of Scientific Research under Grant AFOSR-89-0338 and US Department of Energy under Grant DE-ED02-87ER45301.

References

[1] W.E.Lawrence, S.Doniach, Proc. 12th Intern. Conf. on Low Temp. Phys. ed. by E.Kanda (Academic Press of Japan, Kyoto,1971), p.361.

[2] Yu. M. Ivanchenko, V. L. Belevtsov, Yu. A. Genenko, Yu. V. Medvedev, Sov. J. Low Temp. Phys. (USA) **17**, 1239 (1991). Physica **C 193**, 1992, 291.

[3] V. L. Berezinskii, ZhETF **6**, 1144, (1971).

[4] I. M. Kosterlitz and Thouless, J. Phys. C: Solid State Phys. **5**, L124, (1972).

[5] P. G. De Gennes. Superconductivity of metals and alloys (W. A. Benjamin, New York, 1966).

[6] B. Batlogg, Phys. Today **44**, 44 (1991).

[7] J. C. Phillips, Phys. Rew. B **41**, 8968 (1989).

[8] A. Chang, Z. Y. Rong, Yu. M. Ivanchenko, F. Lu, and E. L. Wolf, Phys. Rew. B **46** to be published (1992).

FIGURE CAPTION

The dependence of energy of a double ring excitation on the ring separation $u = z/2(d_1 + d_2)$ $(F(u) = E_2(\rho, z)/E(\rho))$ for $d_1 = d_2$, $d_2/\lambda_2 = 10^{-3}$, and $\lambda_1/\lambda_2 = 3$.

$\overline{u)}$